THE INFLUENCE OF ROTOR AND FUSELAGE WAKES ON ROTORCRAFT STABILITY AND CONTROL

F.-W. Meyer
and
G. Reichert
Institute of Flight Mechanics
Technical University of Braunschweig, FRG

Abstract

The aerodynamic interference between the wakes of the main rotor and fuselage passing the tail surfaces are to be discussed. A vortex-lattice method is employed to calculate the inviscid flow of the rotor and the development of the separated vortex sheets leaving the rear part of the fuselage. A 3-D-boundary-layer method based on similarity in flow and cross-flow direction is used, to calculate the line of separation. Both, rotor wake and fuselage wake calculations are embedded within a quasi-steady simulation model of the rotorcraft dynamics. Therefore the flow field at the location of the empenage is taken accurately forced by the dynamics of the rotorcraft. Computed flow field and control responses are compared with flight test data. The contributions of the aerodynamics are analysed at major significant flight conditions of helicopters. Time histories of angular velocity rates and a stability chart of the characteristic poles give an overview about the influence of main parameter input.

1. Introduction

Very much interest is growing in forcing the standard of knowledge regarding the theoretical methods for prediction and verification of design goals to new helicopter concepts. This is due to the massive problems of acceptance whether in general (noise) or to the heli-operator for example. Several problem-zones, outlined in Fig.1 are common to all single rotor helicopters. The physical reasons

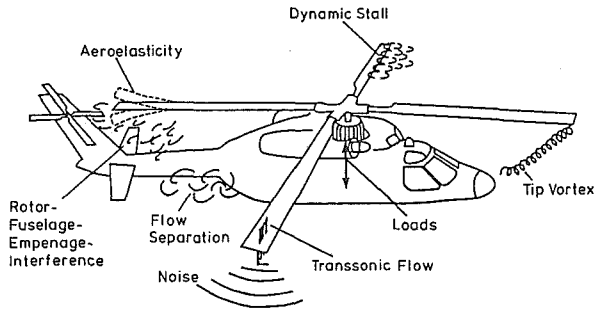

Fig.1 Helicopter aerodynamics

are almost originated from aerodynamic or interactional aerodynamics. Despite of the severe disadvantages, improvements in evaluation of theoretical tools to predict the aerodynamic interaction are made only in the few past years since Clark and Maskew's pioneering work, Ref./1/. The feed back of interactional aerodynamics as interference of rotor and empennage is still a lack of research, Curtis Jr. and Quackenbush /2/ did some theoretical work in this area and of course Sheridan with excessive wind tunnel tests /3/. The main disadvantage in this context is that normally the surfaces of empennage operate in a very complex wake of main rotor and perhaps fuselage as can be seen in Fig.2 performed by the present method (only a

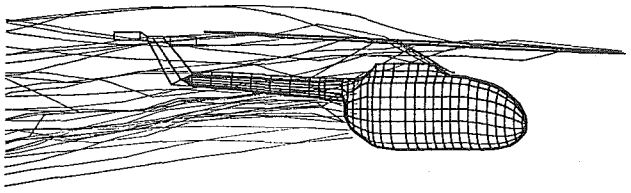

Fig.2 Flow grid pattern, v_k = 25m/s

few stream lines are shown). While larger horizontal tail surfaces are required to provide more angle of attack stability at low and somewhat higher advance ratios (flight speed) the vertical tail surfaces in combination with tail rotor reflect the design requirement to make the rotorcraft directionally stable. Twice, at low and high forward speeds the wake structure borne from rotor and fuselage become responsible to the airloads of tail surfaces including tail rotor. The dynamic pressure at locations of the empennage can have losses up to the half of free stream dynamic pressure as can be seen from flight test results in Fig.3. The dynamic pressure loss centre displacement at empennage is strongly affected by the rotor. The wake amounts due to steady flight state values can be generalized. The wake characteristics and their effects are briefly described in Ref./2/ and /4/. Generally good agreement of the results of present model with flight tests is given

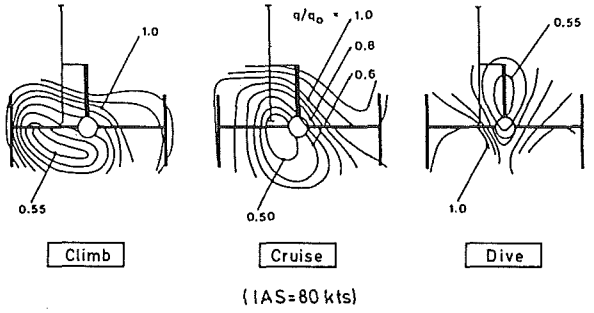

Fig.3 Dynamic pressure losses at tail, Ref./6/

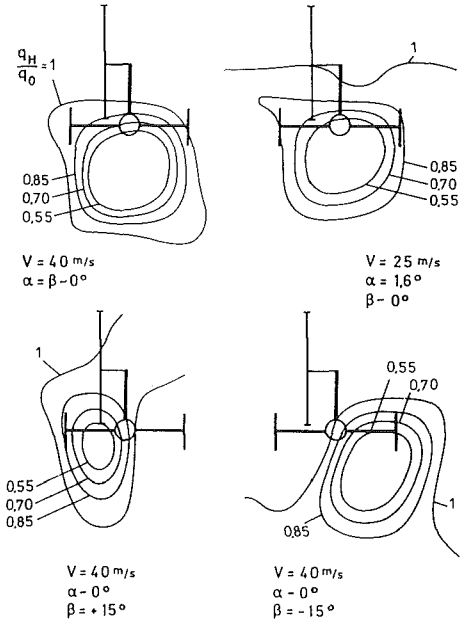

Fig.4 Dynamic pressure losses at tail, present model, Ref./4/

from Fig.4 of Ref./4/ in comparison to Fig.3 here always for steady flight states. But dynamic flights such as maneuver flights or flights with pilots hands off need an unsteady formulation of both wakes from rotor and of course the fuselage and may be rotor hub.

The modelling of massive regions of separated flow in three dimensions as fuselage flow can be treated by methods of discrete vortex dynamics, instead of Navier-Stokes methods, which require much more computer costs and may fail at Reynolds numbers of a few millions . A coupling of the vortex-lattice solution with the solution of boundary layer computation is necessary to define the separation line and feeding turbulence energy.

The extension of the wake model in Ref./4/ to a more sophisticated unsteady one is based upon time stepping procedures in free wake method. This provides the capability of implementing wake lag effects causing phase shifting of acting aerodynamic forces at the tail surfaces. These tail forces must be fed back to the dynamic simulation procedure thus the dynamics and motion of the aircraft depend on the entirely trimmed flight conditions whether descending or climbing. Also aircraft stability is affected due to wake effects.

2. Rotor Flow

As shown by Fig.1 the rotor of a helicopter operates at very different flow conditions. The rotor blades are stressed by the high dynamically airloads, which originate of shocks or fast massive flow separations on the retreating side. Accurate modelling of these nearest flow conditions on rotor blade within the most important physical effects can not be handled by classical potential flow analysis. But the outer flow remains to take place as an ideal incompressible flow. Euler and potential methods are suitable to treat these flow conditions, which includes interference of blade to blade and rotor to fuselage. The flow is characterised as a convectional incompressible flow within embedded small spaced vortices from the rotor blade tips. Even very crude rotor models based upon potential method Ref./1/ with special application of actuator disc theory give relative good results.

Common to all potential methods for modelling rotor flow is the description of the three-dimensional flow by application of Laplaceŝ Equation:

$$\nabla^2\phi = 0 \qquad (1)$$

With the help of Greenŝ Identity the solution of (1) is reduced to a boundary value problem. The numerical computation needs discretisation of the boundary with well fixed boundary values. According to Ref./1/ the rotor is modelled as an actuator disc, see Fig.5 with a connected rotor wake modelled as tubular oriented grid of vortex-lattices.

The appropriate distribution of potential, which contribute to the rotor load and the physical fact, that air mass goes through the rotor disc, leads to the application of dipoles or vortex rings.

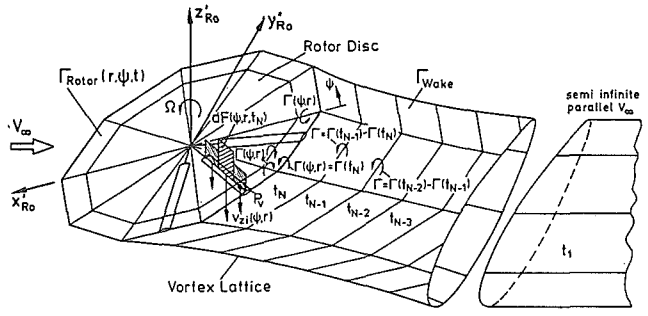

Fig.5 Rotor wake grid

This model is based on vortex segments with constant strength and fictive length. An exact formulation should have further wake connections and wakes distributed along rotor radius because every changing bounded vortex strength value along radial intersections means a connection of free vortex lattice. In this present model only the strong vortex gradient at the rotor blade tip (blade tip path) is conducted through vortex lattices.

The linearity of Laplaces´Equation means the possibility of superposition of particularly solutions of Eq.(1). Representing sources and sinks and dipoles in translational fluid is described by Eq.(2) where two different surfaces exist.

$$\underline{n}\nabla\left(-\frac{1}{4\pi}\int\int_S \frac{\sigma(S_1)}{(S_1,P)}dS_1 + \right. \tag{2}$$

$$\left. + \frac{1}{4\pi}\int\int_S \mu(S_2)\frac{\partial}{\partial n}\left(\frac{1}{r(S_2,P)}\right)dS_2\right) = -\underline{n}\cdot V_\infty$$

With discretization of surface S_1 and S_2 the integral equation changes to a system of algebraic equations. The control points of the panel system are defined as the local center of panel surface. According to Hess /5/ the flat panels with constant dipole strength are redistributed by vortex rings. This is why the Biot-Savart law is applicable to the finite vortex segments with constant strength.

The inner trim loop for calculation of rotor load distribution gives also the rotor downwash (equality of downwash and rotor load) which mean exactly the distribution of boundary values as induced velocity distribution. The induced velocity distribution is given by:

$$\sum_{j=1}^{N}\underline{\underline{A}}_{ij}\underline{\Gamma}_j + \sum_{k=1}^{L}\underline{\underline{B}}_{ik}\underline{\Gamma}_K = \underline{w}_i \tag{3}$$

where bounded (rotor disc) and free (wake) vorticity contribute. The shed vorticity from the outer panel row of the rotor disc is convected each time step towards the wake tube, see Fig.5. For a conservative system equation (3) can be rewritten as follows:

$$\sum_{j=1}^{N}\underline{\underline{A}}_{ij}\underline{\Gamma}_j = \underline{w}_i - \sum_{k=1}^{L}\underline{\underline{B}}_{ik}\underline{\Gamma}_k \tag{4}$$

because the wake conditions are known at time step N-1, and solution of Eq.(4) is possible.

The time step generating rotor wake is obtained by summation of all potentials at time interval dt. The nodes of the free vortex lattice (Free Wake) are derived from Eq.(5):

$$\underline{X}_i^{n+1} = \underline{X}_i^n + (\underline{V}_{i\infty} + \underline{V}_i^n)\cdot\Delta t \tag{5}$$

As long as small time intervals are submitted, even impulsively starting conditions can be simulated. Time variant rotor thrust variations or other flight maneuver non trimmed are possible for simulation in this manner. This means a quasi-steady formulation of the rotor wake. Changing flight states within the defined time intervals are excluded.

3. Fuselage Flow

In the past almost all but today still some helicopter designs look like bluff bodies with rotors. Even for streamlined fuselage shapes there exist massive flow separation induced by rotated crossflow from rotor in case of low forward speeds. At high forward speeds the fuselage is inclined to free stream direction and much more at non-horizontal flights, an important flight domain of helicopters, flow separation occurs.

Considerable share of flight performance and dynamics are due to the fuselage flow problem of the helicopter. What we intend here to show is that the fuselage wake plays an important role for flight dynamics. Therefore the main effects are to be modelled, prediction of the oncoming flow of the tail surfaces.

The outer flow is well known as potential flow. Vorticity is transported from boundary layer behind separation into the vortical wake. These main effects are modelled by many investigators by coupling of vortex-lattice solution with a suitable method of calculating the three-dimensional boundary layer.

Consider the three-dimensional bluff-body separated flow, similarity is shown to a free convected aged shear layer. The outer flow remains as potential flow in the inner region turbulence takes place exclusively. These velocity gradients with high intensity spatial and time depending are only to be modelled by application of Navier-Stokes methods. If any interest is put in small bounded turbulence formation but estimating the averaged velocity components somewhat downstream of separation (locations of tail surfaces) a change is given by application of vortex-lattice methods based upon free wake methods. The flux of flow energy from outer flow initiated by separation of the boundary layer into the inner region can be modelled by vortex-lattices. Flow convection and dynamic pressure loss are well handled but the conservative behaviour disagree to the physical dissipation.

The present fuselage wake model was derived as a quasisteady formulation. Like the rotor flow model here is a time stepping procedure implemented also for handling in the main-frame of a quasi-steady flight simulation code. The quasi-steady formulation of the vortex-lattice is meant as the conditions of connection wake grid to the separation line of boundary layer. Strength of potential, the vorticity and the convection velocity and direction of separating boundary layer are

defined by application of Helmholtz´theorem "conservation of vorticity".

The potential discontinuity at nascent wake grid is taken equal to the momentary vorticity of the boundary layer at separation line. Per time interval there convects the vorticity containing shear layer of separation boundary layer into the nascent wake grid. In order to derive this amount of vorticity, it is suitable to define a control volume of closed region. In general the vorticity is defined by integration of scalar multiplication of bounded line length with velocity:

$$\Gamma = \oint \underline{V} \cdot d\underline{S} \qquad (6)$$

Velocity and line length are known by the state of boundary layer. Eq.(6) changes to $\Gamma = U\,dx$, where U defines the outer flow velocity at edge of boundary layer and dx means the length of control volume at time interval dt. It must be satisfied that the direction of U is perperdicular to the interesting part of separation line.

Placing the first nascent line of wake grid onto the fictive rised separation line with about the boundary layer thickness at point of interest gives automatically the conditions of zero-velocity at body surface. This is what one needs for defining the integration length of Eq.(6). According to Ref./6/ the shear flow is meant as solid rotation. Approximating the separating boundary layer profile linearly changes the definition of profile velocity as follows:

$$\frac{\partial u}{\partial z} = f(z) \cong \frac{du}{dz} = \frac{u_e}{\delta} \qquad (7)$$

and after setting equality the integration of Eq.(6) with circulation of solid body $\Gamma = 2\pi r V$ gives:

$$dx = 2\pi\delta \qquad (8)$$

Open and closed "separation line" can be treated here, a closed one is approximated by connecting a row of straight lines. Fig.6 gives an impression how the fuselage wake model looks like. In order to reduce computer times and costs there is placed a semi-infinite wake grid which connects to the oldest free wake rows well positioned behind the farest tales of rotorcraft. This approximation seems to be with neglecting errors in comparison to whole free wake model in mind the very crude wake modelling.

The coupling of panel method with boundary layer calculation in the quasi-steady domain allows the interaction of viscous and inviscid regions. Here a one-parameter integral method for boundary layer calculation according to Stocks´method Ref./7/ is used. This method is very efficient and requires curvilinear meshes by profile approximation in main flow and crossflow direction.

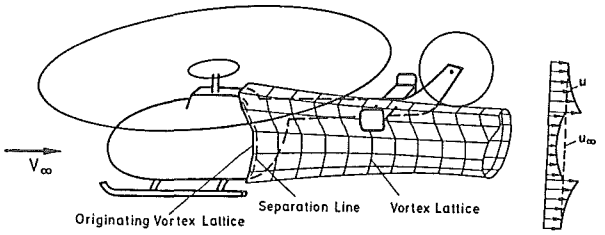

Fig.6 Fuselage wake grid

The application of potential method for calculation of viscous wake flow needs validation with experimental results. In a qualitative manner this is done by comparison of flow conditions at tail locations. Flight test results during development of the BK 117, Ref./8/ are shown in Fig.3. The dynamic pressure distributions, normalized by free stream dynamic pressure depend on actual flight state. The centers of pressure loss indicate losses up to the half of free stream. Influence of tail rotor is shown in case of climb and horizontal flight. Comparing the results of present analysis in Fig.4 a quite good agreement is achieved, additionally the influence of sideward flights is shown. The linear proportionality of dynamic pressure to aerodynamic loads give reason for comparing the distributions of Fig.3,4 as distributions of tail surface effectivness.

4. Quasisteady Simulation Model

The discription of rotorcraft motion as solid body motion is achieved by applying the rules of conservation of translational and rotational momentum. Written in the coordinate system of center of gravity the differential equations of motion are:

$$m_{Ru}\frac{d(\underline{V}_{Kf} + \underline{\Omega}_f \times \underline{r}_f)}{dt} = \sum \underline{F}_f + m_{Ru}\underline{\underline{M}}_{fg} \cdot \underline{g} \qquad (9)$$

$$\frac{d(\underline{\underline{I}}_f \underline{\Omega}_f)}{dt} = \sum \underline{M}_f \qquad (10)$$

The computation of loads and moments of rotor and tail rotor is based upon blade element theory with actuator disc theory and vortex lattice method. Hereby the velocity conditions at the rotor blades are to be estimated which are originated by blade motion, solid body motion and all induced effects of rotor, rotor wake and fuselage flow displacements. Loads of fuselage and empenage are derived by application of look-up tables of aerodynamic coefficients. In case of the vertical and horizontal tail the strip theory is used because of nonsymmetry of the flow about vertical plane. Fig.7 shows the build up of strips and local aerodynamic forces at the tail surfaces. Summation

of all striped lift and drag parts are fed back to the central integration routine. Estimation of the local velocity field is very essential and plus the above mentioned here the induced velocity components due to the fuselage wake are very important. The angle of attack is given by:

$$\alpha_{HLk} = \varepsilon_{HL} + \arctan \frac{w_f - w_{ki} - q_f r_{HL}}{u_f} \qquad (11)$$

for horizontal tail, and

$$\alpha_{SLk} = \varepsilon_{SL} - \arctan \frac{V_f + r_f \cdot r_{SL} + V_{ki} + w_{iHeRo}}{u_f} \qquad (12)$$

for vertical tail, where ε means a inclination; u_f, v_f and w_f are components of solid body translational velocity, q_f and r_f rotational rates respectively. The induced velocities are v_{ki} and w_{ki} but also w_{iHeRo} from tail rotor.

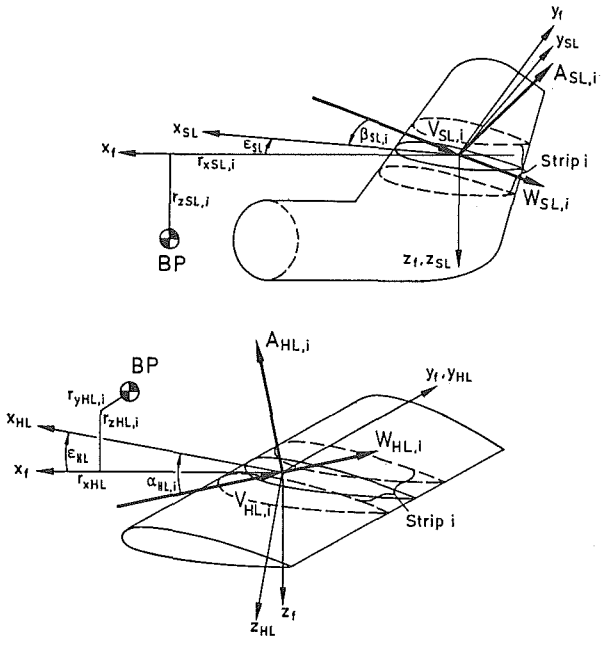

Fig.7 Tail forces

The interference effects are caused not only by interactional aerodynamics of all components of the helicopter. The rotor trim is mainly affected by the moments of solid body which also in fact originate from tail loads.

The heart of the simulation code is the integration routine which solves the equation of motion by application of Runge Kutta method of 4th order. All higher harmonics of rotor blade motion also lagging and torsion are neglegted. Due to the fact that only moderate modes exactly the relevant modes of the solid body are to be investigated here we employed a quasi-steady treatment of the rotor behaviour. The rigid rotor blades are allowed to feather in first harmonic motion without time delay.

Three computation modes are possible: trim mode, stability mode and simulation mode. The overall interaction of airframe with rotor is shown in Fig.8. The interactional aerodynamics and dynamics also control settings are built up as modular functional blocks.

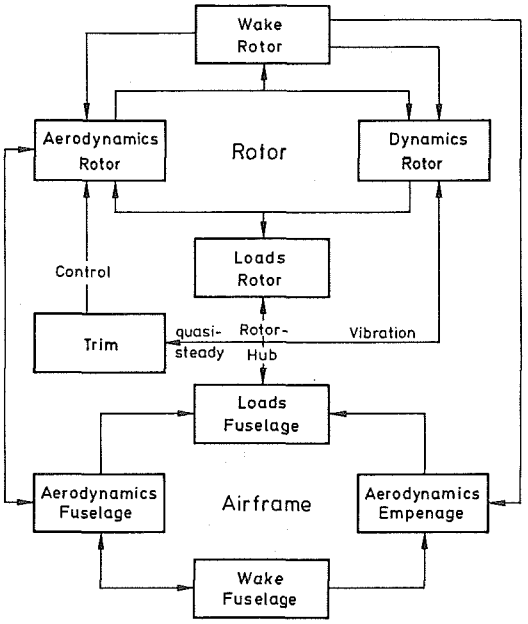

Fig.8 Simulation flow chart

5. Studies on Flight Dynamics

Parameter Spectrum

The results should cover the main influences of interactional aerodynamics which effect the dynamical behaviour of rotorcraft motion. The wide spectrum of parameter variation was captured to the most important ones. Table 1 indicates the range of parameter variation performed in present analysis.

Parameter	Value
Flight speed v_k, v_∞	25; 40; 55 [m/s]
Advance ratio μ	0.11; 0.18; 0.25
Rotor thrust coefficient $c_T = \frac{m * g}{\rho S R U_R^2}$	0.0038; 0.0051; 0.0051
Rate of climb $\dot{H}g(-)$ Climbing	1500; 1000; 0; -1000 [ft/min]
Mass	1700; 2300; 2400 [kg]
Type	Bo 105

Table 1

Pilots get used to fly a helicopter with almost zero bank angle but side slip. The flight test case was analyzed with contribution of side slip. The further investigations were made without side slip.

Velocity Components at Tail Surface Locations

The above mentioned dynamic pressure losses of Fig.3,4 confirm to the flight test measurements of several sources. Recent investigations, see Ref./2/, indicate also a swirl of the wake behind the fuselage with substantial amounts of sideward velocity components. And naturally the rotor downwash and wake deflects the airflow at tail locations downwards but not symmetric to the vertical plane. This is due to the fact that the main rotor loading vary from left to the right side.

Fig.9 is prepared to analyze the individual components of the oncoming flow at horizontal tail by u_{HL}, v_{HL} and w_{HL} at the fin by V_{SL}. Metric length is normalized by span of the tail part. Origin of abszissa for v_{SL} is located at top of the fin. For two important cases the effects of flight path angle is varied from dive ($\dot{H}g$=1500 ft/min) to climb ($\dot{H}g$=-1000 ft/min) In all cases there exists a substantial influence of the wake. At lower forward speeds the main flow directed velocity component u_{HL} shows recovery at climbing flight state, greatest influence of wake here is indicated at steep dive. The downward component w_{HL} shows the most determinative influence of the velocity components of the flight state but influence of the wake is also indicated.

At higher forward speeds the main rotor loading is quite different to the case of lower speeds. Also the kinematic of flight path gives less angle of attack changes at the rotorcraft. For steep dive ($\dot{H}g$=1500ft/min) the right part of horizontal tail operates in cleaner air and efficiency arises. Vertical and sideward velocity components show great dependency on flight state.

Flight Test Cases

From a flight test campaign performed by the Institute of Flight Mechanics at the DLR-Braunschweig, FRG, investigating flight agility of Bo 105 helicopter the special test case of moderate cruising with zero flight path angle is depicted to validate present model. A slight (ß =4-5°) right sideward flight is given. Fig.10,11 show the time histories of control responses. A double step input of main rotor and tail rotor collective pitch is given, also for flight test. Another model output is drawn within the plots which is based upon modelling the influence of main rotor downwash by applying an interference

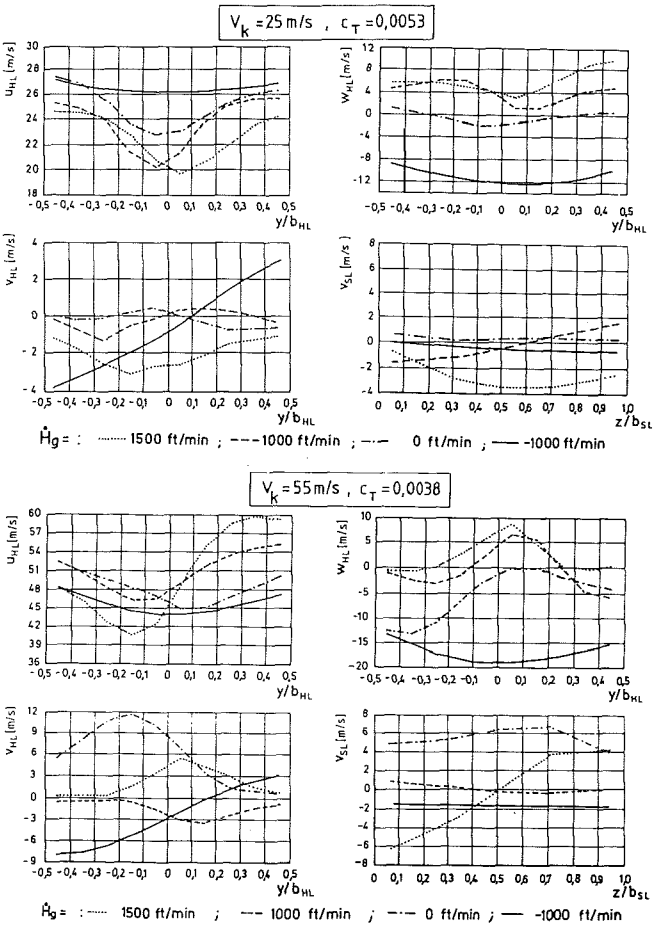

Fig.9 Velocitiy components at tail

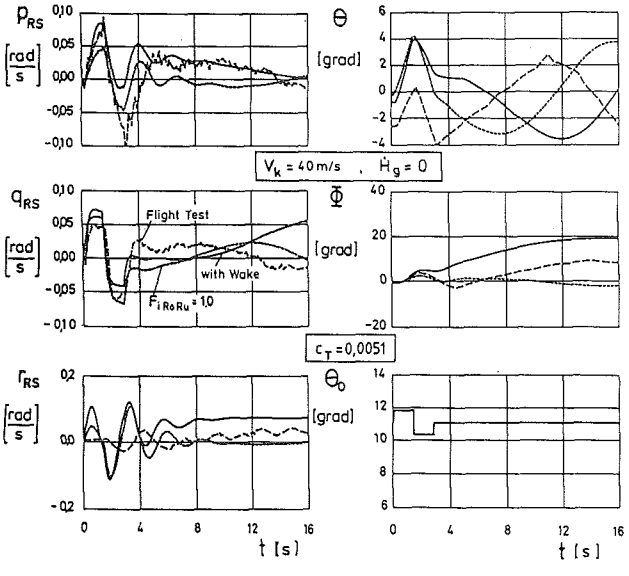

Fig.10 Control responses, comparison with flight test

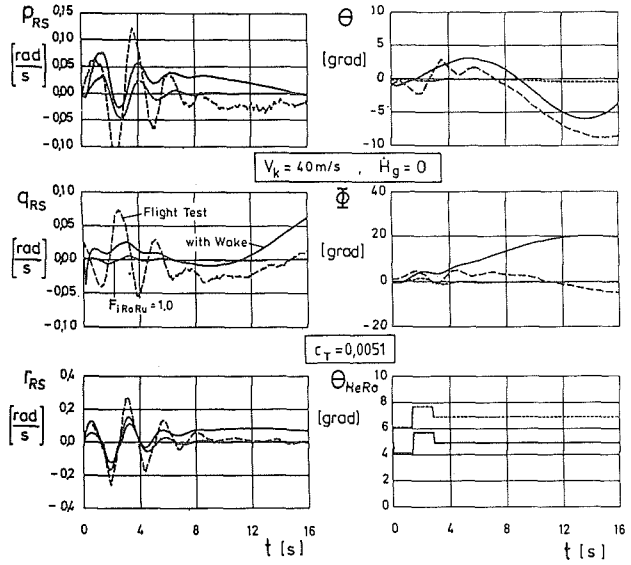

Fig.11 Control responses, comparison with flight test

factor. The factor mentioned here indicates the addition of averaged rotor downwash to the vertical velocity component at tail locations. Comparing to this model version the wake influence shows slight destabilising effects in many cases with more agreement to the baseline of experiment. Overall the angular velocity rates and attitudes of pitch and bank angle are more or less estimated by the flight simulations.

Parameter Variation

The influence of varying flight states to the control response of the Bo105 helicopter is shown in Fig.12-15. First of all there exists a phase shifting in yawing and pitching caused by the wake when comparing the plots with different flight path angle. Additionally there is a slight overshooting of pitching in case of heavier weight of rotorcraft. The influence of flight speed is shown in Fig.14 at slight dive and heavy loaded main rotor.

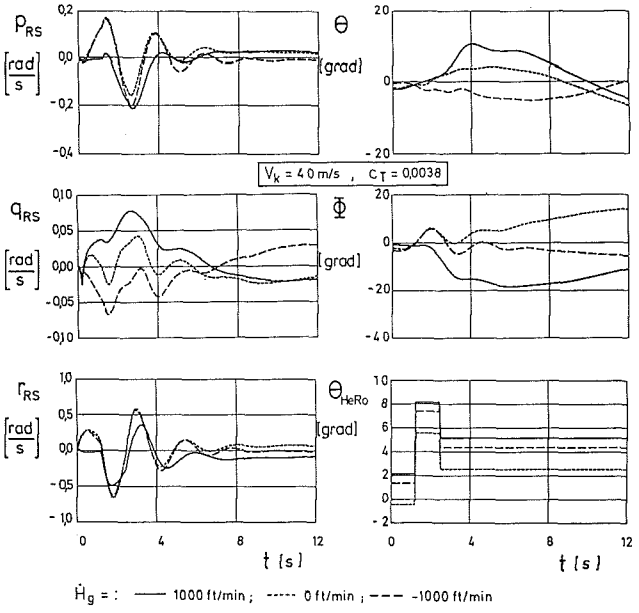

Fig.13 Control responses, influence of flight path angle

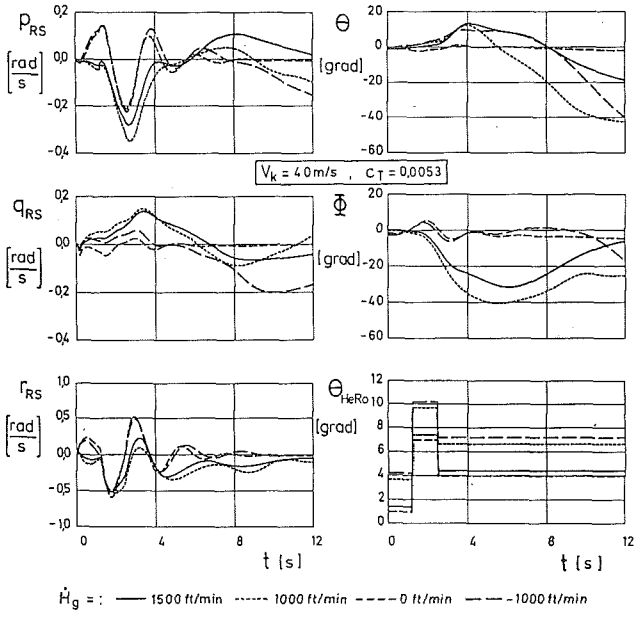

Fig.12 Control responses, influence of flight path angle

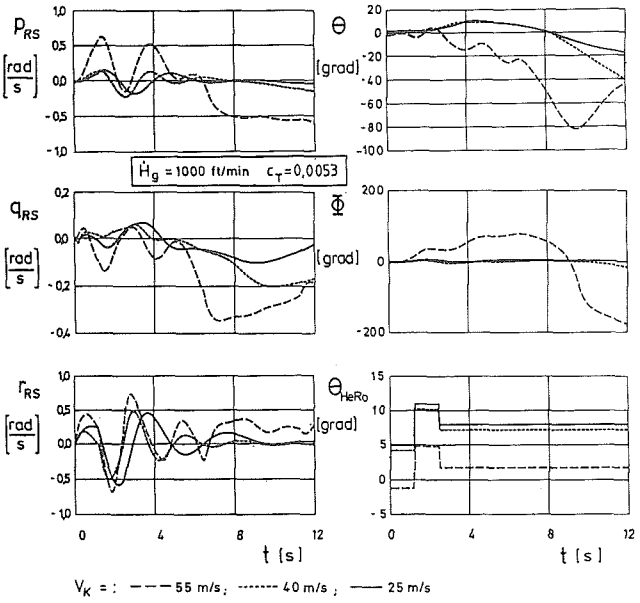

Fig.14 Control responses, influence of flight speed

Normally the responses are affected by the forward speed attitude. The stimulated dutch roll mode in case of high forward speed shows reduced damping up to unstable conditions. The phugoid mode is indicated by the response of pitching angle attitude. Although the need of longer simulation time is evident the beginning of phugoid motion can be depicted from Fig.12,13 where less pitching mode is shown for horizontal flight condition: another reason which can only be explained by the complex structure of the wake.

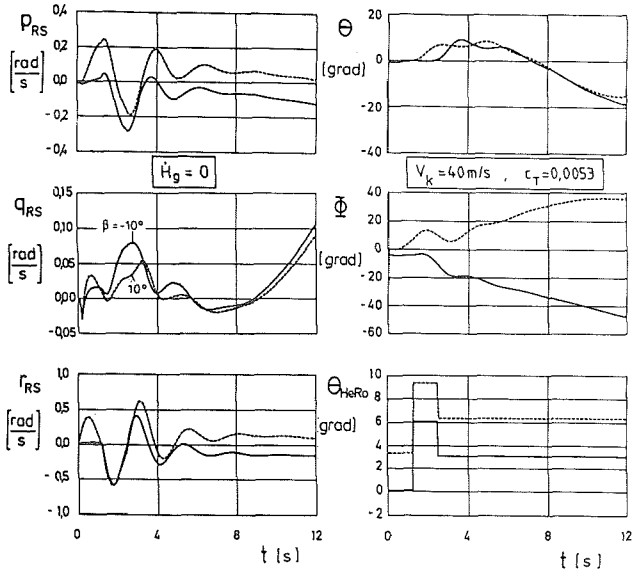

Fig.15 Control responses, influence of sideward flight

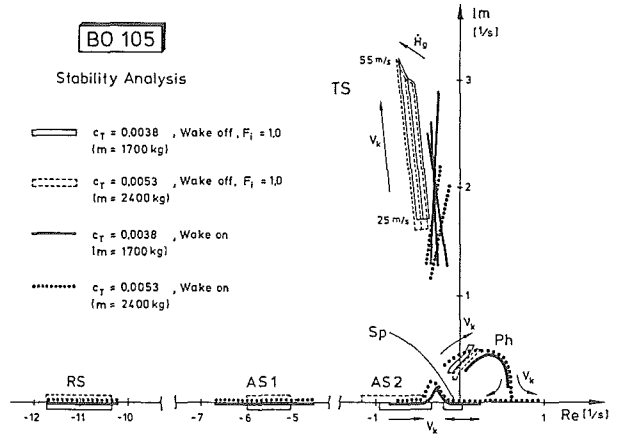

Fig.16 Stability chart

Effects of wake at sideward flights are shown in Fig.15. The trimmed side slip angle varys from ß =-10° to ß =+10° (nose left). A slight phase shifting occurs for rolling and yawing motion. Clean air impinges the tail because the side slip angles are high enough whether left or right slip. Different damping ratios can not be recognized.

6. Stability Analysis

Finally the body motion of the rotorcraft was analysed in the mainframe of interesting flight mechanic standpoint. Therefore a number of cases have to be considered. Fig.16 shows the location of poles depending on weight, forward speed and flight path angle drawn as a stability chart. The classical modes of roll, short period, spiral, phugoid and dutch roll motion are well estimated by both model versions. Overall there is a clear identification of destabilising wake effects on dutch roll and phugoid. This effect arises if heavy loaded main rotor is considered. This seems to be clear of the more induction of rotor downwash and wake effects in case of heavier loaded rotor. The results are made with zero side slip flight simulation and better behaviour should be expected at slight side slipping.

7. Conclusions

* The general features of the influence of average rotor downwash onto the tail effectivness gives quite good results of control responses.

* More accurate calculation of the induced flow field by applying coupling methods of panel and boundary layer methods give considerable chance for better modelling of wake influence.

* The main important parameters as weight, forward speed and flight path angle also side slip angle have influence on the wake effects.

* Results from the present study provide an insight into the complex interaction phenomena.

* The design of new helicopter concepts for special IFR-approval can have restrictions of stability. Accurate prediction with the present model can save several design loops.

* Rotorcraft identification procedures yet have lack of modelling wake induced effects. The present model can help open some doors to these problems.

8. References

/1/ Maskew, B.; Clark, D.R.: Study for Prediction of Rotor/Wake/Fuselage Interference Part I: TR, NASA CR 177340,1985

/2/ Curtiss Jr.,H.C.; Quackenbush, T.R.: The Influence of the Rotor Wake on Rotorcraft Stability and Control. 15th ERF Amsterdam, 1989

/3/ Sheridan, P.F.; Smith, R.P.: Interactional Aerodynamics - A New Challenge to Helicopter Technology. 35th Annual Forum of AHS, 1979

/4/ Meyer, F.-W.: Rotor-Rumpf-Leitwerks-Interferenzen beim Hubschrauber. DGLR-Jahrestagung, 1990

/5/ Hess, J.L.: Calculation of Potential Flow about Arbitrary Three-dimensional Lifting Bodies. Rep. No. MDC J5679/01 Douglas Aircraft Company,1972

/6/ Huber, H.; Polz,G.: Studies of Blade to Blade and Rotor-Fuselage Tail Interferences. AGARD Fluid Dynamics Panel Specialists Meeting on Prediction of Aerodynamic Loads on Rotorcraft, 1982

/7/ Stock, H.-W.: Integralverfahren zur Berechnung dreidimensionaler laminarer und turbulenter Grenzschichten an Tragflügeln und Rümpfen. DORNIER-Endbericht Nr. 77/51B,1977

/8/ Faulkner, A.: Kloster, M.: Lateral-Directional Stability: Theoretical Analysis and Flight Test Experience. 9th ERF, 1983

/9/ Behr, R.: Programm VLM1, Berechnung der Interferenzen zwischen freien Wirbelschichten und Tragflügeln, Institut für Luftfahrttechnik und Leichtbau, Universität der Bundeswehr München, 1987